Derivation and Evaluation of a 2nd Order Model of Cantilever Beam Vibration

Bryson Rogers
Samantha Devapiriam

University of Southern California AME 341b
Mechoptronics

Lab Day: Wednesday February 24, 2021

Abstract

A 2nd order model of the displacement of the free end of a cantilever beam was derived using a damped oscillator model. Real beam vibration was measured and used to derive empirical, system-specific parameters for the proposed model. The shapes, amplitudes, and frequencies of the real and semi-theoretical responses were compared to evaluate the merits of the proposed model. The proposed model matched the qualitative shape of the beam response. The amplitude of the semi-theoretical response was within $\pm 12\%$ of the actual amplitude for 500 cycles, and this error decreased if fewer cycles were considered, longer after beam perturbation. The semi-theoretical response phase stayed within $\pm 180°$ for about 277 cycles.

1. Introduction

A cantilever is a horizontal beam with one fixed end and one free end and a uniform mass distribution, as shown in Figure 1.

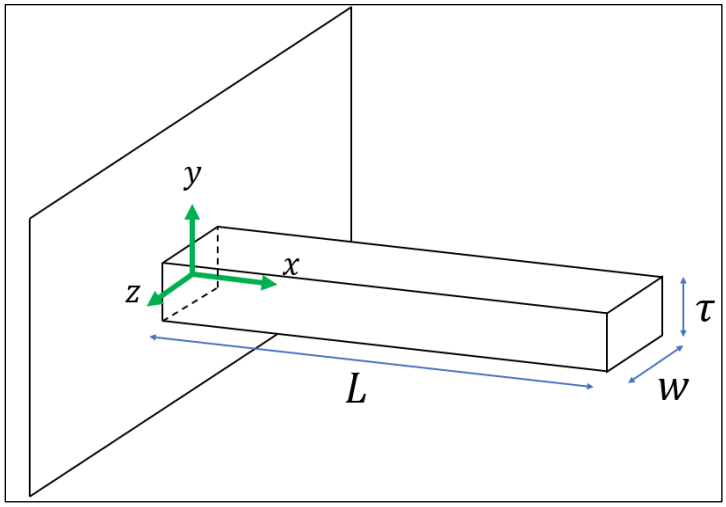

Figure 1. Diagram of a cantilever beam of length L, thickness τ, and width w

It is assumed that beam length is much greater than beam thickness, i.e. $L \gg \tau$. It has been shown in continuum mechanics literature that free vibration of a cantilever beam is governed by Equation 1

$EI\frac{\partial^4 y(x,t)}{\partial x^4} = -\rho A\frac{\partial^2 y(x,t)}{\partial t^2}$	$I = \frac{\pi}{4}w\tau^3$	1

where $y(x,t)$ is vertical displacement as a function of position x and time t, I is the second moment of area of the beam cross section about the z axis, E is the Young's Modulus of the beam material, and A is cross sectional area [1]. Solving Equation 1 for $y(x,t)$ yields an infinite series of sinusoids, where the i^{th} sinusoid ("mode") has amplitude A_i and angular frequency ω_i. The first mode, or "fundamental" mode, has the largest amplitude A_0 and lowest frequency ω_0. The fundamental frequency ω_0 depends on the geometry and material of the beam. The lowest-order modes dominate the vibration of the beam, as A_i decreases by orders of magnitude with each successive mode.

The above mathematical description of cantilever beam vibration is exact for an ideal beam, but it is often impractical to find A_i and ω_i for real cantilever beam systems. This model does not account for non-ideal factors in real systems, such as fluid resistance, energy loss through the mounted end and wiring, or mismatch between theoretical and actual material or geometry. To address these limitations of the ideal theoretical model above, this paper proposes and evaluates a simplified 2nd order model and accompanying system ID methodology.

2. Proposed Model

A 2nd order model was developed to provide a simplified mathematical description of cantilever beam vibration. The beam system was modelled as a damped oscillator located at the tip of the beam, as shown in Figure 2.

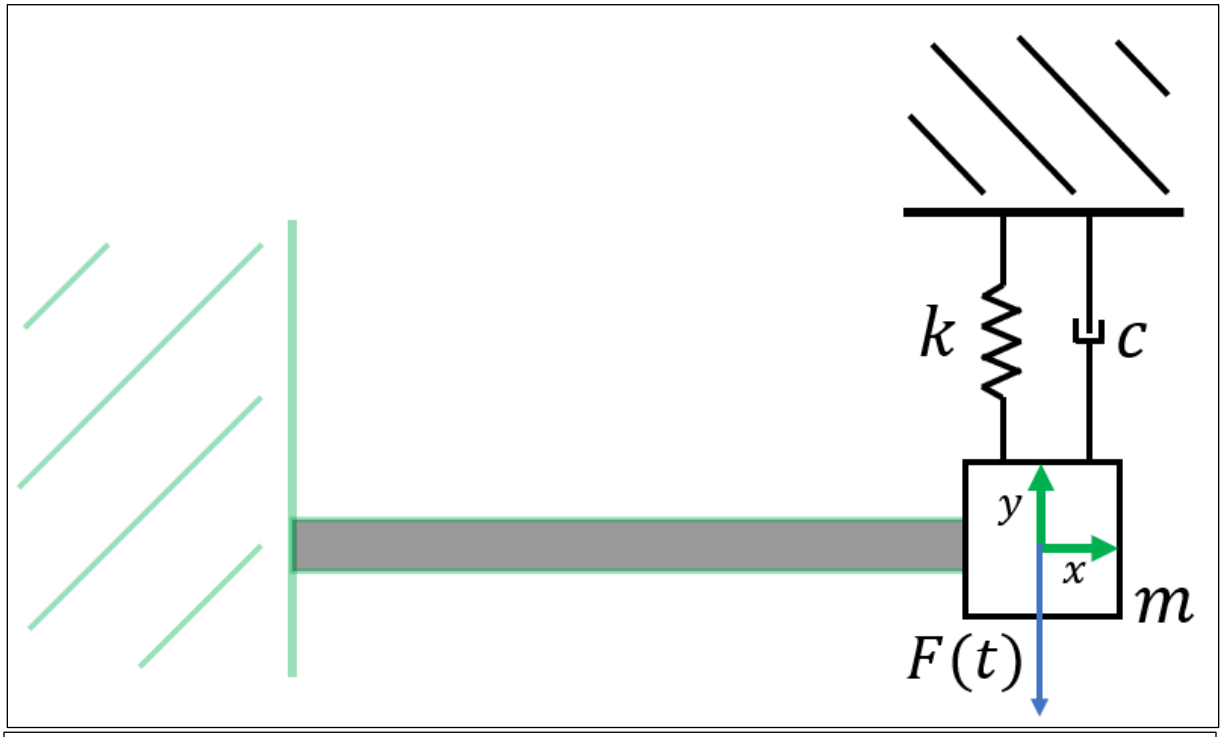

Figure 2. Diagram of hypothetical damped oscillator proposed to model vibration at end of beam, where k is the spring constant, c is the damping coefficient, m is the oscillator mass, and $F(t)$ is applied force

Note that the damped oscillator in Figure 2 is not physical; it is mathematical construction used to model the beam as a 2nd order system. The motion of the damped oscillator is governed by Equation 3, a 2nd order differential equation of motion.

$$m\ddot{y} + c\dot{y} + ky = F(t)$$	2

When the damped oscillator model is applied to the beam system, m, c, and k are referred to as *lumped parameters*, and represent the inertial properties, energy dissipation, and elasticity of the beam system, respectively. The validity of Equation 2 as a model for beam vibration is determined by the ability to capture all relevant physics of the system by adjusting the lumped parameters. Multiple assumptions were made to model the beam as a damped oscillator:

1. Only the displacement at the end of the beam is of interest
2. Only vibration at the fundamental frequency is of interest
3. The displacement at the end of the beam is purely vertical (in the y direction)

Equation 2 was rearranged to obtain the more standard Equation 4

$\ddot{y} + 2\zeta\omega_n\dot{y} + \omega_n y = F(t)/m$	3

$\omega_n = \sqrt{k/m}$	4	$\zeta = c/2\sqrt{mk}$	5

where ω_n is the natural frequency and ζ is the damping ratio. ω_n is the angular frequency of the system in the hypothetical case of zero damping (zero energy loss). ζ is a dimensionless value that characterizes the rate of decay of system response due to energy loss. For a physical system, ζ is always greater than zero. Together, ω_n and ζ determine the exponential and oscillatory behavior of a 2nd order system.

Solutions of Equation 3 for $y(t)$ take the form of Equation 7

$y(t) = ke^{-\zeta\omega_n t}e^{\pm i\omega_n t\sqrt{1-\zeta^2}}$	6

where i is the imaginary unit and k is some constant (k is intermediate in this derivation and is not of interest). The form of the solution $y(t)$ depends on the value of ζ:

1. If $\zeta > 1$, then $\sqrt{1-\zeta^2}$ is imaginary, and the second exponential term in Equation 6 has real exponents.
2. If $\zeta < 1$, then $\sqrt{1-\zeta^2}$ is real, and the second exponential term in Equation 6 has complex conjugate exponents

The beam used in the experimental setup was made of an aluminum alloy with a damping ratio $\zeta \cong 0.0035$ (other materials, particularly metals, similarly have $\zeta < 1$) [2] It was thus assumed that $\zeta \ll 1$, which corresponds to the second case above. The solution $y(t)$ therefore takes the form of Equation 8

$y(t) = \underbrace{e^{-\zeta\omega_n t}}_{exp.\ decay} * \underbrace{(A\cos\omega_d t + B\sin\omega_d t)}_{oscillation}$	7
$\omega_d = \omega_0\sqrt{1-\zeta^2}$	8

where ω_d is the damped frequency of the beam and A and B are constants. Because damping is always present in a real physical system, the observed frequency of oscillation is the damped frequency ω_d, not the hypothetical undamped frequency ω_0. A and B are determined by initial conditions, which were chosen to be $y(0) = y_0$ and $\dot{y}(0) = 0$. These initial conditions correspond to the experimental setup, discussed in Section 3.1. Applying these initial conditions to Equation 7, after some algebra, yields Equation 10.

$A = x_0$	$B = x_0\zeta/\sqrt{1-\zeta^2}$	9

It was already assumed that $\zeta \ll 1$. Therefore, $\zeta/\sqrt{1-\zeta^2} \ll 1$ and $B \ll A$. Considering this, it was assumed that the contribution of $B\sin\omega_d t$ in Equation 7 is negligible and can be ignored. With this assumption, Equation 7 can be simplified to Equation 11.

$y(t) = y_0 e^{-\zeta\omega_n t}\cos\omega_d t$	10

Equation 10 is the proposed 2nd order model of cantilever beam vibration. Numerical values of ω_n and ζ, which are system-specific, are needed to obtain a complete expression for $y(t)$. To obtain

values for ω_n and ζ and evaluate the validity of the proposed model, experimental beam vibration data was gathered using the methods detailed in Section 3.

3. Materials and Methods

A cantilever beam system was constructed in lab, real beam vibration data were gathered, and experimental values for ω_n and ζ were determined to evaluate the capability of Equation 10 to model real cantilever beam vibration. This method of using experimental data to calculate parameter values yields a system-specific semi-theoretical model, and is referred to as "system ID."

3.1 Experimental Setup

A diagram of the experimental setup is provided in Figure 3.

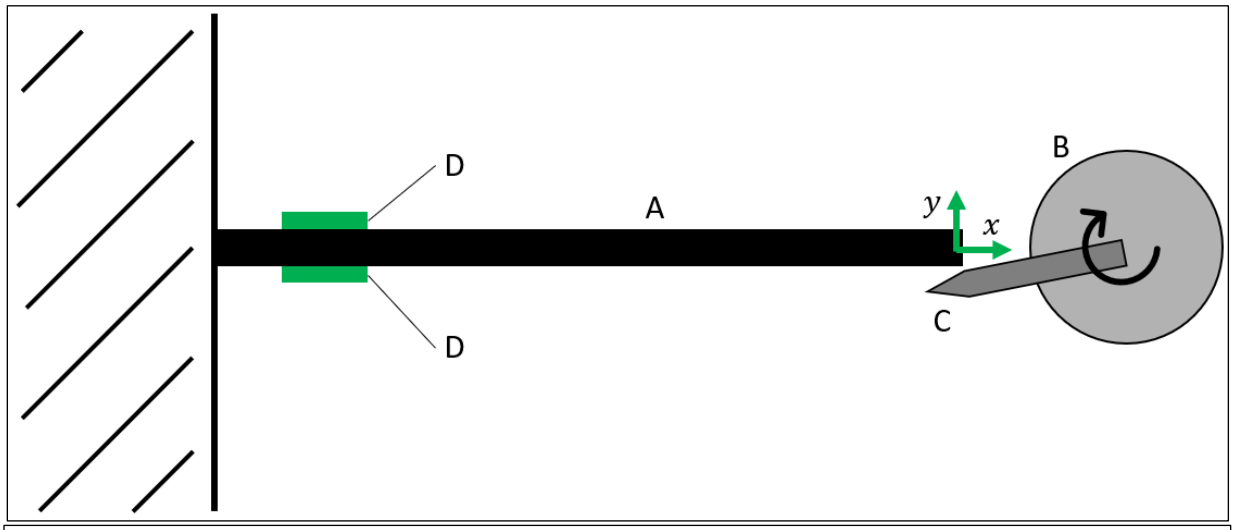

Figure 3. Major components of the experimental setup: an aluminum alloy beam (A) with one fixed end and one free end, a stepper motor (B) and dial (C) used to vibrate the beam, and two strain gauges (D) adhered to the top and bottom of the beam

One end of an aluminum alloy beam was rigidly mounted and the other was left free. The dimensions of the beam are provided in Table 1.

Table 1. Dimensions of beam [mm]

Length L	360 ± 1
Thickness τ	4.8 ± 0.1
Width w	9.6 ± 0.1

A stepper motor with a protruding dial was placed at the free end of the beam as shown in Figure 3. The end of the beam was given an initial displacement $y(0) = y_0$ by rotating the motor in small increments until the dial pushed the end of the beam up and out of its equilibrium position. To initiate beam vibration, the motor was rotated further to release the beam from the dial. The rotation of the dial imparts a nonzero initial velocity to the end of the beam. However, it was assumed that this initial velocity was negligible, such that the assumption $\dot{y}(0) = 0$ used to derive A and B in Equation 9 is valid. Two strain gauges were adhered to the top and bottom of the beam near the mounted end (the exact distance to the end of the beam is inconsequential). The strain gauges were

attached to a strain gauge circuit. The strain gauge circuit output voltage $E(t)$ was used to indirectly measure $y(t)$, the vertical displacement of the end of the beam as a function of time. The strain gauge circuit and method used to measure $y(t)$ is described in Section 3.2.

3.2 Measurement of Beam Displacement using Strain Gauges

Vertical displacement at the end of the beam $y(t)$ was not measured directly. It was instead measured indirectly via strain gauges. The local longitudinal strain at the top and bottom of the beam near the mounted end (ie. at the locations of the strain gauges in Figure 3) is proportional to the vertical displacement at the free end, i.e. $\epsilon_x \propto y$ [3]. ϵ_x was measured using strain gauges.

A strain gauge, shown in Figure 4, exhibits a change in resistance across its leads in response to strain parallel to its wire switchbacks [4].

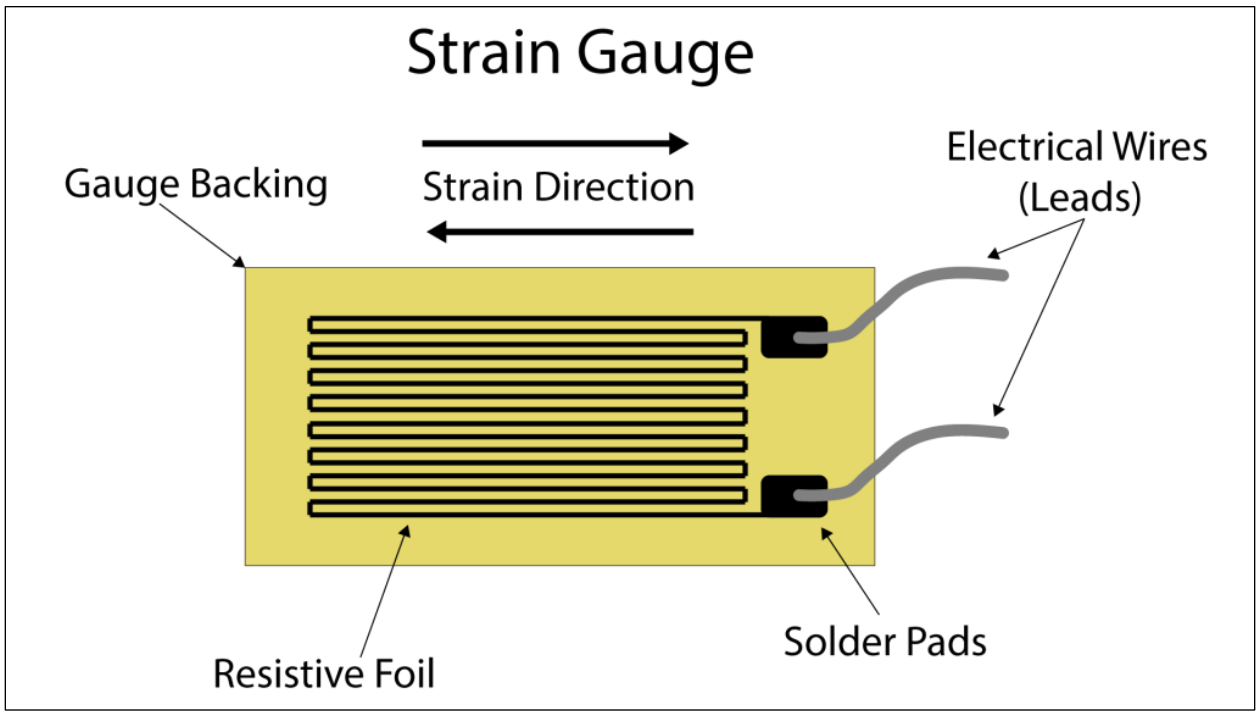

Figure 4. Diagram of a basic strain gauge, which exhibits a change in resistance in response to a strain in the "Strain Direction"

The change in resistance δR as a function of strain ϵ is governed by Equation 12

$$\delta R(\epsilon) = R_0 F \epsilon \quad (11)$$

where R_0 is the resistance when $\epsilon = 0$ and F is an empirically-derived constant. A single strain gauge provides limited capability to measure ϵ accurately because F is highly sensitive to changes in temperature and $|\delta R|$ is on the order of the typical resolution of a digital multimeter. To address these shortcomings (high sensitivity to temperature and low sensitivity to strain), two strain gauges arranged in a Wheatstone bridge circuit were used.

A Wheatstone bridge, shown in Figure 5 is an arrangement of four resistors connected to a DC voltage source.

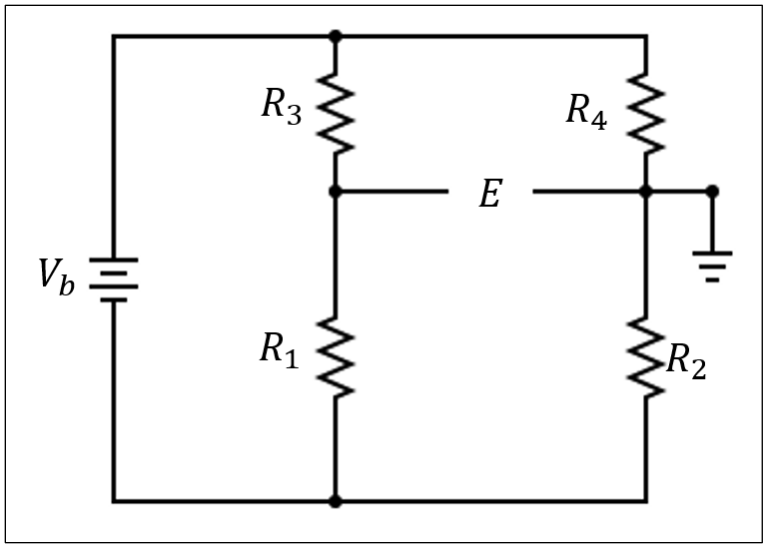

Figure 5. A generic Wheatstone bridge circuit with 4 resistors, a DC power supply V_b, and a potential difference E across its arms

If the resistances across the left and right arms of the Wheatstone bridge are unequal, there is a potential difference E between the two arms, as shown in Figure 5. If $R_1 = R_2$, then E is determined by Equation 13

$$E = V_b \frac{R_1(R_3 - R_4)}{(R_1 + R_3)(R_1 + R_4)} \quad (12)$$

where V_b is the supplied DC voltage. Note that if $R_3 = R_4$, the resistance across each arms is equal, and Equation 12 yields $E = 0$, as expected.

Figure 6 shows the Wheatstone bridge in the experimental setup, in which two strain gauges R_{SG1} and R_{SG2} replace R_3 and R_4 in Figure 5.

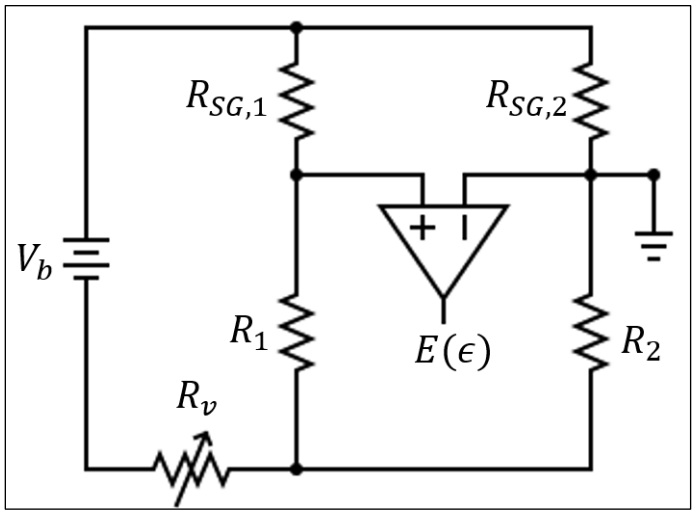

Figure 6. Strain gauge circuit used in lab to indirectly measure $y(t)$. A potential difference $E(\epsilon)$is generated in response to strain and amplified for measurement

R_{SG1} corresponds to the strain gauge on top of the beam and R_{SG2} corresponds to the strain gauge on the bottom of the beam. R_{SG1} and R_{SG2} are functions of strain and temperature, as described by Equations 14 and 15

$R_{SG1}(\epsilon, T) = R_{SG1,0} + \delta R_{\epsilon,1} + \delta R_{T,1}$	13
$R_{SG2}(\epsilon, T) = R_{SG2,0} + \delta R_{\epsilon,2} + \delta R_{T,2}$	14

where $R_{SGi,0}$ is the strain gauge resistance at some baseline temperature and $\epsilon = 0$, δR_ϵ is the change in resistance due to strain, and δR_T is the change in resistance due to deviation from the baseline temperature. Two identical strain gauges were selected such that $R_{SG1,0} = R_{SG2,0} = R_{SG,0}$. Because the strain gauges were adhered to the top and bottom of the beam, the local strains at each gauge are equal and opposite; therefore, $\delta R_{\epsilon,1} = -\delta R_{\epsilon,2} = \delta R_\epsilon$ [3]. It was assumed that the temperatures of both strain gauges were the same at all times; therefore $\delta R_{T,1} = \delta R_{T,2} = \delta R_T$. It was also assumed that that $\delta R_\epsilon, \delta R_T \ll R_1, R_{SG,0}$. Given these conditions and assumptions, it can be shown that the voltage difference $E(\epsilon)$ between the arms of the experimental Wheatstone bridge setup takes the form of Equation 16.

$E(\epsilon) = \underbrace{\left[-2V_b \frac{R_1}{\left(R_1 + R_{SG,0}\right)^2} F\right]}_{constant} \epsilon$	15

Equation 15 shows that the two-strain gauge Wheatstone bridge circuit shown in Figure 6 resolves the aforementioned limitations of using a single strain gauge to measure ϵ:

- The potential difference $E(\epsilon)$ can be amplified, unlike the change in resistance δR of a single strain gauge, and therefore measured more accurately
- The coefficient "2" in Equation 15, which follows from using two strain gauges, increases the sensitivity of $E(\epsilon)$ to ϵ
- $E(\epsilon)$ in Equation 15 has no dependence on temperature due to algebraic cancellation of $\delta R_{T,1}$ and $\delta R_{T,2}$.

A differential op-amp and a variable resistor R_v were included in the strain gauge circuit. $E(\epsilon)$ was amplified using the op-amp for more accurate measurement, and R_v was used to balance small discrepancy between the resting resistances of the arms of the circuit.

Equation 15 suggests that $E(\epsilon)$ is linearly dependent on ϵ, as all terms in the brackets are constant. It was assumed that $\epsilon \propto y$, and Equation 15 shows that $E \propto \epsilon$; therefore, $E \propto y$. E was thus used as a proxy for displacement y, and was used to calculate ω_n and ζ, as detailed in Section 3.3.

3.3 Calculation of Model Parameters ω_n and ζ

Natural frequency ω_n and damping ratio ζ determine the oscillatory and exponential decay characteristics of the proposed 2nd order model. ω_n and ζ were calculated using experimental beam vibration data then used to compare $E_{exp}(t)$ to $E_{model}(t)$.

Calculation of ζ

If $t = nT$, where t is time, T is the period of ω_d, and n is an integer number of cycles, then Equation 10 can be rewritten as Equation 17

$E(n) = E_0 e^{-\zeta \omega_n nT}$	16
$T = t_{tot}/N$	17

where t_{tot} is the total time of response observation and N is the number of oscillations during t_{tot}. Solving Equation 16 for ζ and applying the assumption $\sqrt{1-\zeta^2} \cong 1$ yields Equation 19, which was used to calculate experimental values of ζ as a function of n.

$\zeta(n) = \frac{\ln(E_0/E(n))}{\omega_n nT}$	18
$\zeta_{avg} = \frac{\sum_{n=1}^{N} \zeta(\mathrm{n})}{N}$	19

Calculation of ω_n

Solving Equation 8 for ω_n and using the result of Equation 18 for ζ yields Equation 21, which was used to calculate experimental values of ω_n as a function of n.

$\omega_n(n) = \frac{2\pi}{T\sqrt{1-\zeta^2}}$	20
$\omega_{n,avg} = \frac{\sum_{n=1}^{N} \omega_{\mathrm{n}}(\mathrm{n})}{N}$	21

The assumption $\sqrt{1-\zeta^2} \cong 1$ was not applied in Equation 20 because small discrepancy between $\omega_{n,exp}$ and $\omega_{n,model}$ causes phase shift to accumulate between $E_{exp}(t)$ to $E_{model}(t)$ over many cycles.

4. Results and Discussion

Beam vibrations were measured over a 19-second interval, and the vibration data was used to calculate experimental values of ω_n and ζ according to the proposed 2nd order beam model.

Figure 7 compares the actual beam vibration to the semi-theoretical model. The experimental data and semi-theoretical model exhibit the same qualitative exponential decay and oscillatory behavior.

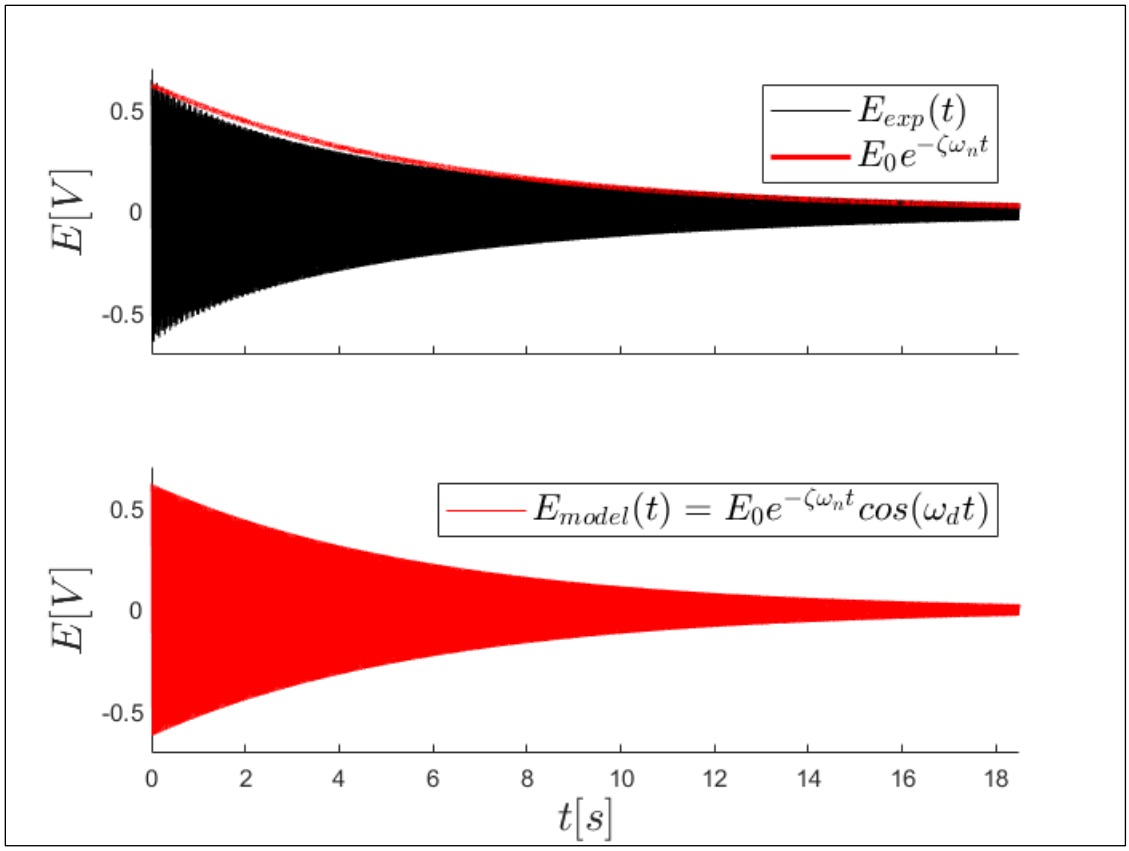

Figure 7. Comparison of actual beam response (top) and semi-theoretical model (bottom). The semi-theoretical exponential bounding function is plotted over the actual beam response for comparison. Note: the curves appear to be continuous areas due their high frequency of oscillation

$\zeta(n)$ was calculated at several n over the observed interval using Equation 18 and was plotted in Figure 8.

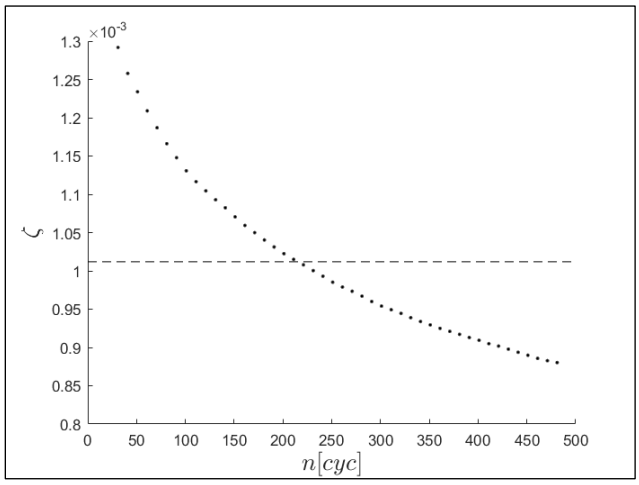

Figure 8. ζ decreases asymptotically as n increases

The proposed model predicts a constant value for ζ, but ζ was found to decrease as a function of n. In the proposed model, ζ was defined in Equation 5 by the lumped parameters m, k, and c. The variation of ζ as a function of n may result from nonlinear physics that could not be fully described by the lumped parameters alone. In particular, it was assumed that energy dissipation is linearly proportional to beam end velocity by the damping coefficient c. This assumption likely becomes less accurate as n decreases, when higher order modes and higher beam velocity cause energy dissipation to be larger than the model predicts. The mean ζ across the entire time interval of data collection was calculated using Equation 19: $\zeta_{avg} = 0.0010 \pm 0.0002$. The uncertainty was determined via the t-estimator method [5].

The value of ω_n varied relatively little as a function of n. Across the 19-second interval of data collection, $\omega_{n,avg}$ =165.1086 $\pm$ 0.0003 rad/s, and the standard deviation of ω_n was 2E-5. This agrees with the model's prediction of a constant ω_n.

The power spectrum of the measured beam vibrations is presented in Figure 9.

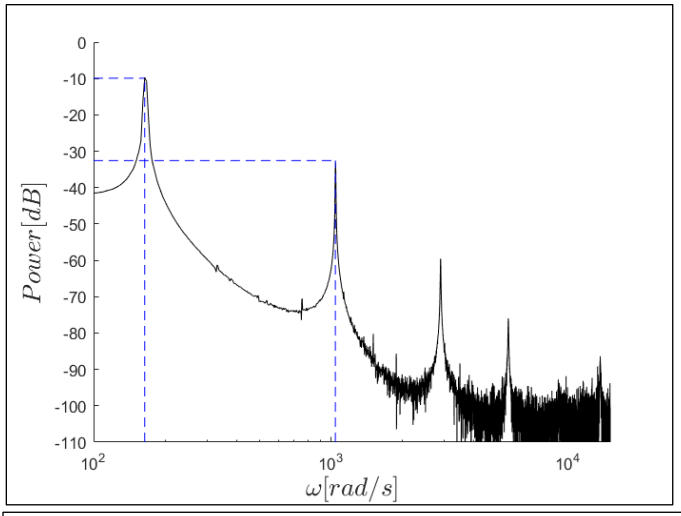

Figure 9. Power spectrum of the measured beam vibration; decreasingly intense, higher frequency modes are visible as peaks

The power spectrum contains 5 peaks, the frequencies and powers of which are provided in Table 2.

Table 2. Frequencies and powers of the 5 peaks visible in the beam vibration power spectrum

Peak i	ω_i ($\pm$1) [rad/s]	P_i [dB]
0	164	-9.9
1	1044	-32.6
2	2897	-59.7
3	5583	-76.0
4	13618	-86.7

The first peak corresponds to ω_0, the fundamental frequency of the beam. ω_0 was equal to ω_d, which is expected because ω_d was calculated using the observed period of the beam vibration. The

ratio of the intensities of the first and second frequencies (P_1/P_0) was 0.0054, which supports the assumption that the beam response is dominated by vibration at the fundamental frequency.

Over many cycles, a time discrepancy accrued between corresponding peaks of the measured and semi-theoretical vibrations (the measured peaks lead the semi-theoretical peaks). The time difference Δt (normalized by the period T) between corresponding peaks is plotted as a function of cycle number n in Figure 10.

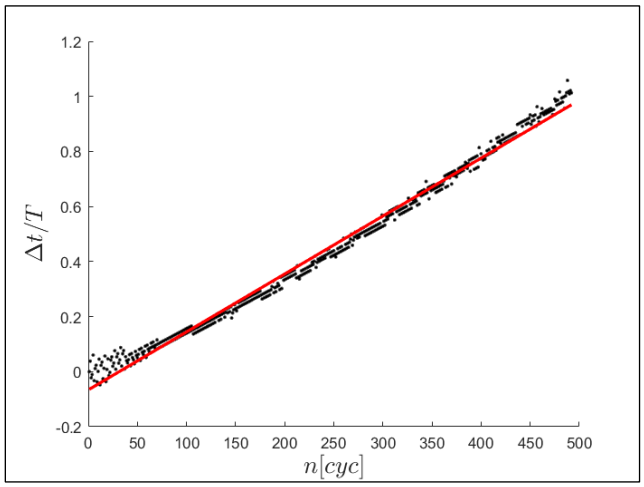

Figure 10. The time delay between corresponding peaks of the measured and semi-theoretical vibrations increased approximately linearly as a function of n

$\Delta t/T$ increased approximately linearly as a function of n; a linear regression of slope 0.0021 fit the data with an R-square value of 0.996. The relative difference between the beam's fundamental frequency ω_0 and the semi-theoretical damped frequency ω_d was therefore $\omega_0 - \omega_d = 0.0021\omega_0 = 0.347 rad/s$.

The error between amplitudes of the corresponding peaks of the measured and semi-theoretical vibrations were calculated as a percent and plotted in Figure 11.

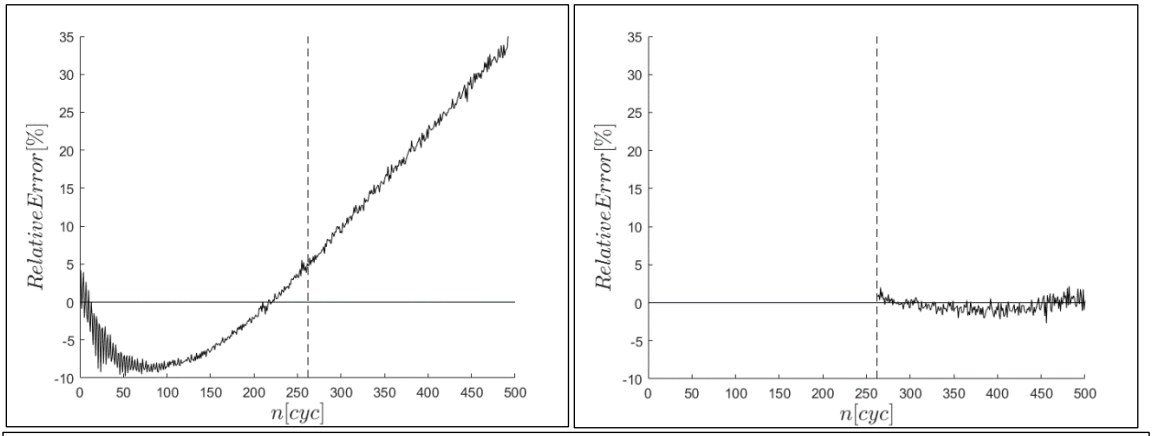

Figure 11. Relative amplitude error as a function of n. Left: $E_0 = E(t = 0s)$. Right: $E_0 = E(t = 10s)$

Figure 11 compares the amplitude error when the above analysis is performed starting 0 seconds after beam perturbation, and 10s after beam perturbation. The average magnitude of the error was far less in the $t_0 = 10s$ case: 0.76% as compared to 12% over the entire modelled interval. This

suggests that the accuracy of the proposed model increases as the length of the time interval it is modelling decreases, and as the time since perturbation increases.

5. Conclusion

A 2nd order model of cantilever beam vibration was derived by modelling the beam as a damped oscillator. It was assumed that the beam oscillated only at the fundamental frequency, and that only displacement at the end of the beam was of interest. A semi-theoretical response $y(t)$ was determined via "system ID": experimental values of ω_n and ζ were calculated using measured beam vibrations then used calculate $y(t)$.

System ID is a useful methodology because on system characteristics must be neglected to empirically derive of parameter values. All system attributes (material properties, geometric irregularity, air resistance, damping effects of sensor wires, etc.) are accounted for in the actual beam response. Many of these factors are difficult and mathematically-intensive to account for in a purely theoretical model derivation.

The proposed 2nd order model matched the qualitative exponential and oscillatory behavior of the cantilever beam vibration. The amplitude of the semi-theoretical response was within $\pm 12\%$ of the actual amplitude for 500 cycles, and this error decreased if fewer cycles were considered, longer after beam perturbation. The semi-theoretical response phase stayed within $\pm 180°$ for about 277 cycles. These findings suggest that the proposed semi-theoretical 2nd order model is an acceptable approximation of cantilever beam vibration depending on the requirements of the application for which one applies this model. These findings also suggest that system ID is an effective and simple (relative to purely theoretical derivation) method to derive system-specific, empirical values for cantilever beam model parameters. Further work or literature review is necessary to determine the applicability of system ID to other systems and models.

References

[1] S. Whitney, "Vibrations of Cantilever Beams: Deflection, Frequency, and Research Uses", *http://emweb.unl.edu/*, 2021. [Online]. Available: http://emweb.unl.edu/Mechanics-Pages/Scott-Whitney/325hweb/Beams.htm. [Accessed: 06- Mar- 2021].

[2] H. Mevada and D. Patel, "Experimental Determination of Structural Damping of Different Materials", *Procedia Engineering*, vol. 144, pp. 110-115, 2016. Available: 10.1016/j.proeng.2016.05.013.

[3] Theory and Design for Mechanical Measurements, Figliola & Beasley (2010) Wiley

[4] T. Nachazel, "What is a Strain Gauge and How Does it Work?", *Michigan Scientific Corporation*, 2021. [Online]. Available: https://www.michsci.com/what-is-a-strain-gauge/]. [Accessed: 07- Mar- 2021].

[5] B. Gerstman, t Table, San Jose State University, July 2020. [Online]. Available: https://www.sjsu.edu/faculty/gerstman/StatPrimer/t-table.pdf

Appendix: Matlab Script

```
% AME 341b Mechoptronics E12
% Bryson Rogers
% Model of Beam Bending
clear; clc; close all;

% NOTE file naming conventions:
% sampleFreq_numSample_signalShape_domain.txt

%% Process Trace Data
fileName = fullfile('E12 Raw
Data','1000Hz_20000n_beam_time.lvm');
trace1kHz = dlmread(fileName,'\t');
eOut = trace1kHz(:,2); t = trace1kHz(:,1);

[peak,peakTime] = findpeaks(eOut,t); %Find value and time
of each voltage peak
firstPeakIndex = 273; %first peak after twang at index 273
n0 = 20;%+262; %20->t0, 262->t=10s
t0 = peakTime(firstPeakIndex+n0);
tInd = (t >= t0) & (t <= peakTime(end));
t = t(tInd); eOut = eOut(tInd);
t = t - t0; %set time of e0 to 0 s
eOut = eOut - mean(eOut); %subtract mean voltage

%% Period T
% Method calculate each quantity as a function of time
using a 'rolling
% average' over 21 cycles

%Calculate Period T
eOutPos = eOut>0; %number corresponds to positive, 0
corresponds to negative or 0
signChange = xor(eOutPos(1:end-1),eOutPos(2:end)); %logical
vector: 1=sign change, 0=no sign change
totSignChange = sum(signChange);
numCyc = (totSignChange-1)/2; %total sign changes is
roughly 2*number of cycles + 1
T = t(end)/numCyc;

%% Extract time and magnitude of oscillation peaks
[peak,peakTime] = findpeaks(eOut,t);
```

```
peak = [eOut(1);peak]; peakTime = [0;peakTime]; %Include
first peak (t=0,eout=e0)
peakTime = peakTime(peak>0); peak = peak( peak>0 );
%Exclude negative peaks (result of higher order
oscillation)

%Exclude peaks that result from higher order oscillations
for i = 2:length(peakTime)
    if peakTime(i) - peakTime(i-1) < 0.6*T
        if peak(i) >= peak(i-1)
            peak(i-1) = 0;
        else
            peak(i) = 0;
        end
    end
end
peakTime = peakTime(peak>0); peak = peak( peak>0 );
T2 = t(end)/(length(peak)-1);
% nIndex = 1:length(peakTime); %%%%

%% Damping Ratio zeta
%Calculate zeta(t) as a running average over 21 cycles
e0 = mean(peak(1:5));
n = 31;
j=1;
zeta = zeros(1,floor( (length(peak) - 20)/10)-1);
nVec = length(zeta);
while n<= length(peak) - 10
    runningTotal = 0;
    for i = -10:10
        runningTotal = runningTotal + log(e0/peak(n+i)) /
(2*pi*(n+i)); %calculate zeta for each cycle
    end
    zeta(j) = runningTotal/21; %avg zeta over 21 cycles
    nVec(j) = n;
    n=n+10; j=j+1;
end

zetaMean = mean(zeta);

% n13s = floor(13/T2);
% e013s = mean(peak(n13s:n13s+3));
% zeta13s = zeros(1,length(nIndex));
% for i = n13s+1:length(nIndex)
```

```
%     zeta13s(i) = log(e013s/peak(nIndex(i))) ./
(2*pi*(nIndex(i)-n13s));
% end
% zeta13sMean = mean(zeta13s(zeta13s>0));
%% Natural Frequency w0
%Calculate w0 as a running avg over 21 cycles
w0 = zeros(1,length(zeta));
for i = 1:length(w0)
    w0(i) = (2*pi) / (T2*sqrt(1-zeta(i)^2));
end
w0Mean = mean(w0); wd = 2*pi/T2;


%% Model
tModel = linspace(0,t(end),15000);
e0Model = e0*exp(-zetaMean*w0Mean*tModel).*cos(wd.*tModel);
expModel = e0*exp(-zetaMean*w0Mean*tModel);
% e013sModel =  e013s*exp(-
zeta13sMean*w0Mean*tModel).*cos(wd.*tModel);
%% Peak Time Discrepancy deltaT as a function of n
[modelPeak,modelPeakTime] = findpeaks(e0Model,tModel);
modelPeak = [e0(1),modelPeak]; modelPeakTime =
[tModel(1),modelPeakTime];
deltaT = zeros(1,length(modelPeakTime));
nIndex = 1:length(deltaT);
for i = 1:length(modelPeakTime)
    deltaT(i) = (modelPeakTime(i) - peakTime(i))/T2;
end

scatter(nIndex, deltaT,'k.');hold on;
[linReg,S] = polyfit(nIndex,deltaT,1);
dtdn = linReg(1); %discrepency between frequencies omegad
and fundamental freq of beam
rMatrix = corrcoef(nIndex',deltaT');
rSqr = rMatrix(2);
plot(dtdn*nIndex + linReg(2),'r','LineWidth',2)
xlabel('$n [cyc]$','interpreter','latex','FontSize',16);
ylabel('$\Delta t/T$','interpreter','latex','FontSize',16);
hold off;
%% Frequency Response
fileName = fullfile('E12 Raw
Data','7000Hz_15000n_beam_power.lvm');
spec7kHz = dlmread(fileName,'\t');
freq = spec7kHz(:,1)*2*pi; P = spec7kHz(:,2);
```

```
dFreq = (freq(2)-freq(1))/2;
P0P1ratio = 10^(22.67273/10);

semilogx(freq,P,'k');
hold on;
plot(164.209*[1,1],[-150,-9.7112],'b--')
plot([0.00001,164.209],-9.91117*[1,1],'b--')
plot(1043.9*[1,1],[-150,-32.5839],'b--')
plot([0.00001,1043.9],-32.5839*[1,1],'b--')
%Format Plot
xlabel('$\omega[rad/s]$','interpreter','latex','FontSize',1
6);
ylabel('$Power[dB]$','interpreter','latex','FontSize',16);
xlim([100 15000]); ylim([-110 0]); box off;

%% Amplitude Response
hold off;
relError =  zeros(1,length(nIndex));
for i = 1:length(nIndex)
    relError(i) = 100*(peak(i) - modelPeak(i)) / peak(i);
end

%plot(nIndex,relError,'k')
plot(nIndex,relError,'k') %+262

hold on;
%plot(e013sModel)

%Format Plot
plot([0,500],[0,0],'k-'); box off;
plot([262,262],[-100,100],'k--');
xlabel('$n [cyc]$','interpreter','latex','FontSize',16);
ylabel('$Relative Error
[\%]$','interpreter','latex','FontSize',16);

xlim([0 500]); ylim([-10 35]);

%% Plots
hold off

%Zeta vs n plot
zetaError = std(zeta)*1.684;
scatter(nVec,zeta,'k.'); box off; hold on
plot([0,500],[zetaMean,zetaMean],'--k');
```

```
xlabel('$n[cyc]$','interpreter','latex','FontSize',16);
ylabel('$\zeta$','interpreter','latex','FontSize',16);
xlim([0 500]); ylim([.8E-3 1.3E-3]);

%omegan vs n plot
omegaError = std(w0)*1.684; hold off
omegaSTD = std(w0);
scatter(nVec,w0,'k.'); hold on; box off
plot([0,500],[w0Mean,w0Mean],'--k');
xlabel('$n[cyc]$','interpreter','latex','FontSize',16);
ylabel('$\omega _n
[rad/s]$','interpreter','latex','FontSize',16);
%xlim([0 18.5]); ylim([165.1971 165.1973]);

% Exp data vs exponential model curve

subplot(2,1,1); hold on;box off;
plot(t,eOut,'k'); %experimental data
plot(tModel,expModel,'r','LineWidth',2)
legend({'$E_{exp} (t) $','$E_0 e^{-\zeta \omega _n t}
$'},'interpreter','latex','Location','northeast','FontSize'
,14)
xticklabels('');
ylabel('$E[V]$','interpreter','latex','FontSize',16);
xlim([0 18.5]); ylim([-0.7 0.7]);

subplot(2,1,2);
plot(tModel,e0Model,'r');box off;
xlabel('$t[s]$','interpreter','latex','FontSize',16);
ylabel('$E[V]$','interpreter','latex','FontSize',16);
xlim([0 18.5]); ylim([-0.7 0.7]);
legend({'$E_{model}(t)=E_0 e^{-\zeta \omega _n t}
cos(\omega _d
t)$'},'interpreter','latex','Location','northeast','FontSiz
e',14)
```